A spatially explicit model of patchy stomatal responses to humidity

J. W. HAEFNER, T. N. BUCKLEY & K. A. MOTT

Department of Biology and Ecology Centre, Utah State University, Logan, UT 84322–5305, USA

ABSTRACT

Stomata of leaves can exhibit either temporally stable, spatially homogeneous behaviour or complex spatial and temporal dynamics, depending on environmental and physiological conditions. To test the ability of accepted physiological mechanisms to describe these patterns, we developed a simple, spatially explicit model of stomatal responses to humidity that incorporated hydraulic interactions among stomata. Model results showed qualitative agreement with experimental evidence for a number of phenomena: (1) at high humidities, whole-leaf steady-state conductance is a monotonic function of humidity; (2) the initial stomatal response following a perturbation in humidity is in the direction opposite to the final response, and (3) spatial dynamics include patch formation and self-organization similar to that observed in actual leaves. These comparisons do not eliminate other explanations, but do suggest that novel mechanisms need not be invoked to explain the diversity of spatial and temporal patterns of stomatal behaviour in leaves.

Key-words: humidity; oscillations; patchy; spatially explicit model; stomata.

INTRODUCTION

Models of stomatal functioning vary in their approach and objectives. Detailed mechanistic models of single stomata can predict both steady-state and non-steady-state responses, and can serve as powerful investigative tools to provide insight into these responses (Delwiche & Cooke 1977; Rand & Ellenson 1986). However, these models are generally complex and contain a large number of leaf-specific variables that are difficult or impossible to measure accurately. Empirical models that predict steady-state stomatal conductance as a function of environmental parameters (e.g. Ball, Woodrow & Berry 1987; Leuning 1995) can be useful tools in scaling from single-leaf responses to canopy processes. These models, however, provide little insight into the mechanisms underlying the responses, and they typically do not predict the kinetic aspects of stomatal responses or non-steady-state responses such as oscillations. Furthermore, empirical

Correspondence: James W. Haefner. E-mail: jhaefner@biology. usu.edu

models are unable to address the most difficult problem posed by scaling: interactions among small-scale units (e.g. individual stomata within a leaf).

Interactions among individual stomata have not been an issue in the past because of studies showing an approximately normal distribution of stomatal apertures (Laisk 1980), which suggest that individual stomata behave independently. However, recent studies have shown that the distribution of stomatal apertures over a leaf surface is not always normal, and that under some circumstances the mean aperture of stomata in certain areas of a leaf may be very different from that of the rest of the leaf. This phenomenon has been termed patchy stomatal closure (see Terashima 1992; Pospisilova & Santrucek 1994 for reviews); it is not detectable with standard gas-exchange techniques but has been demonstrated using $^{14}[C]CO_2$ uptake, vacuum infiltration of leaves, and images of chlorophyll fluorescence. Studies using these techniques show that stomatal patches can vary in size from 1 to many millimetres and are usually delimited by veins. The pattern of patches over a leaf may be static or dynamic, and some patches may oscillate between high and low conductance (Cardon, Mott & Berry 1994; Weis & Siebke 1995). Patchy stomatal closure has been shown to occur under a variety of environmental conditions including low humidity (Terashima 1992; Pospisilova & Santrucek 1994).

These observations are consistent with the hypothesis that some form of interaction or communication among stomata leads to synchronized stomatal movements in localized areas of the leaf at low humidities. Other hypotheses are possible, for example that there is a central, controlling signal that induces synchronized dynamics. To our knowledge, there is no evidence in support of this idea. Our working hypothesis, which is explored through the use of a computer simulation model, is that local interactions produce the global pattern. Previously, Rand *et al.* (1982) and Rand & Ellenson (1986) extended the single stoma model of Delwiche & Cooke (1977) and examined one-dimensional systems of coupled stomata. These studies, while insightful, did not consider (1) the more complicated and realistic two-dimensional system, (2) ionic interactions between the epidermis and guard cells, or (3) the effects of veins on spatial patterns. As a result, none of the existing models of stomatal functioning predicts the observed, two-dimensional, patchy stomatal dynamics. Nevertheless, it seems likely that the mechanism resides in the epidermis or the mesophyll immediately adjacent to the

epidermis because the patterns of stomatal patches can be different for the upper and lower surfaces of amphistomatous leaves (Mott, Cardon & Berry 1993). The purpose of this study was to explore the hypothesis that simple hydraulic interactions can produce coordinated behaviour for stomata within an areole, and could therefore cause the complex spatial and temporal patterns of stomatal conductance that have been observed in leaves at low humidities. To accomplish this goal, we constructed a spatially explicit model of stomatal responses to humidity that was based on generally accepted mechanisms for the functioning of single stomata, using hydraulic mechanisms to produce interactions between stomata. Qualitative aspects of the model output were then compared to stomatal responses in leaves.

MATERIALS AND METHODS

Experimental procedures

The gas-exchange data presented in this paper were acquired with a standard single-pass gas-exchange system that has been described previously (Mott, Cardon & Berry 1993). Briefly, gas of a known composition was produced from pure N_2, O_2, CO_2 and H_2O using electronic mass flow controllers. This gas was delivered at a known rate to a leaf chamber, and the effluent gas was analysed for differences in H_2O vapour and CO_2 concentrations. Leaf temperature was measured using a fine-wire chromel constantan thermocouple. Light was provided by a 150 W Xenon bulb and delivered to the leaf surface using fibre-optic bundles (PFD = 1000 μmol m^{-2} s^{-1}). All experiments were carried out at an ambient CO_2 concentration of 350 μmol mol^{-1}.

Images of chlorophyll fluorescence were acquired and analysed as described previously (Daley *et al.* 1989; Mott 1995). Briefly, a leaf in a gas-exchange chamber was illuminated with light filtered to remove wavelengths above 700 nm. The leaf was exposed to 1 s pulses of high light (PFD = ≈5000 μmol m^{-2} s^{-1} also filtered to remove wavelengths above 700 nm) at regular intervals. During each pulse of high light, the leaf was imaged using a CCD camera that was filtered to detect only light above 700 nm. Images of chlorophyll fluorescence were analysed with reference to a maximum fluorescence image that was acquired on a dark-adapted leaf, and in the final images brightness is negatively correlated with stomatal conductance (see Daley *et al.* 1989; Mott *et al.* 1993; Mott 1995, for details). These changes in chlorophyll fluorescence can be caused by physiological changes in the mesophyll or by stomatally induced changes in intercellular CO_2 concentration. For the low humidity treatment in this experiment, stomatal conductance changes are the most likely explanation (see Cardon *et al.* 1994; Bro, Meyer & Genty 1996; Mott 1995 for further discussion of this topic). Our experiments were conducted at an O_2 concentration of 0·02 mol mol^{-1} to maximize the changes in fluorescence intensity (Daley *et al.* 1989).

Model description

Our purpose here is not to elaborate the most mechanistically realistic model possible, but rather to investigate the effects of simple representations of stomata in a complex spatial lattice that includes veins. As a result, we will ignore many phenomena known to influence stomata (e.g. light, CO_2, temperature, etc.) and use linear relationships in place of non-linear ones. By simplifying, we hope to identify mechanisms sufficient to explain the spatial patterns. We do not mean to imply that other mechanisms are not important or unable to produce similar patterns.

Spatial structure

The model is a system of finite difference equations defined on a rectangular lattice. These equations describe the dynamics at each lattice grid point, as well as the interactions among neighbouring grid points. This approach is similar to cellular automata, which are discrete in space, time and state, but it differs in that we allow an infinite number of states for each grid location. Figure 1 illustrates the components of the lattice and the hydraulic flows among the biological entities defined at each grid location. Each grid location is termed a stomatal unit (SU) and is composed of a guard cell pair and its surrounding epidermal tissue (Fig. 1). An areole is a set of SUs surrounded but not divided by veins (heavy lines in Fig. 1). The arrows in Fig. 1 indicate flows among neighbouring water compartments (guard and epidermis cells).

Assumptions

The model is a mathematically simple implementation of the following biological assumptions.

(1) Stomatal aperture is a linear combination of epidermal and guard cell turgor pressures. Direct measurements of stomatal aperture as a function of guard cell and epidermal turgor by Meidner & Edwards (1975) revealed a relationship of this form. A detailed analysis of stomatal mechanics by Sharpe, Wu & Spence (1987) yielded the same conclusion. Epidermal turgor has relatively greater effect on aperture than does guard cell
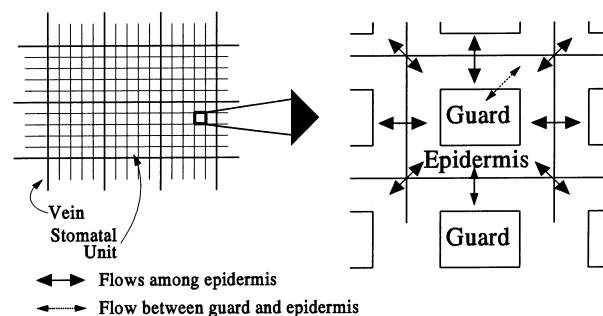
Figure 1. Spatial structure of the model. The left panel shows the lattice of veins and interacting stomatal units. The right panel shows a single stomatal unit as composed of a pair of guard cells and epidermal tissue. Arrows indicate pathways of water flow.

turgor (Sharpe *et al.* 1987), and their importance varies randomly among stomata and across the leaf surface.

(2) Water flows from the xylem to an evaporating site within the leaf. Most proposed feedback mechanisms for stomatal responses to transpiration rate incorporate the concept of an evaporating site that experiences a reduction of water potential proportional to the transpiration rate (Schulze 1994; Mott & Parkhurst 1991). This idea is consistent with pressure probe studies demonstrating that mesophyll and epidermal water potentials decrease as the water vapor mole fraction deficit (Δw) is increased, while xylem water potential stays relatively constant (Nonami & Schulze 1989).

(3) The evaporating site is in close hydraulic contact with the epidermis. The exact path that water follows from the xylem to the evaporating site(s) and the relative amounts of water that evaporate from the mesophyll and the epidermis are unknown. There is good evidence that the epidermis supports considerable evaporation (Shackel & Brinckmann 1985), or is at least in close hydraulic contact with the site of evaporation in the mesophyll (Nonami & Schulze 1989). In the current model, the precise site of evaporation was not specified, but it was assumed to be in close hydraulic contact with the epidermis. In essence, the water potentials (Ψs) of the epidermis and mesophyll were considered to be uniquely and positively related.

(4) The osmotic pressure of the guard cells is a function of the water potential (or turgor) of the evaporating site. This assumption provides a means for stomata to respond to Δw. At present, there is no generally agreed upon mechanism for stomatal responses to humidity. Most data are consistent with feedback regulation of guard cell turgor in response to changes in the water status of the evaporating site (Cowan 1977; Schulze 1994), and the available evidence supports active regulation of guard cell solute content in response to humidity changes (Losch & Schenk 1978). Our model incorporates these conclusions by assuming that the steady-state value of guard cell osmotic pressure increases with elevated epidermal turgor pressure. Previous models of stomatal dynamics (e.g. Delwiche & Cooke 1977) do not include this phenomenon.

(5) Water moves among water compartments in the leaf in response to water potential gradients. Water must flow from the xylem to the point(s) of evaporation for each stoma. Since there is no evidence for exclusive water pathways for each stoma, we assume that water leaving the xylem will flow to each evaporating site based on its water potential.

Equations

We studied the behaviour of the following set of difference equations, which were based on the assumptions outlined above. Each SU of the lattice (Fig. 1) contained two compartments: the guard cells and the epidermis. The water potential of the epidermal compartment (Ψ_e) was calculated in each

time step as a function of (i) the water potential during the previous time step, (ii) the flow of water to and from adjacent water compartments, and (iii) the water loss through transpiration (changes in the volume of the guard cell compartment are considered negligible with respect to the volume of the epidermal compartment, and are neglected). In this simple model, water flow was not modelled explicitly, but the critical state variable, water potential, was considered to be linearly related to water content and thus to volume. Consequently, water potential is determined from transformed water flow equations [assumptions (2) and (3)]:

$$\frac{d\Psi_e^i}{dt} = a\left(F_e^i - E^i\right). \tag{1}$$

The index i refers to a specified SU in the lattice. Ψ_e^i is the water potential of the epidermis in SU i, F_e^i is water flow into or out of the epidermis of the ith SU, E is transpiration rate, and a is a constant factor converting volume to water potential.

To simplify computations, we convert Eqn 1 to finite difference form with an arbitrarily defined time step of unity. The basic model becomes

$$\Psi_{e,t+1}^i = \Psi_{e,t}^i + aF_{e,t}^i - aE_t^i. \tag{2}$$

The numerical values of the parameters implicitly define the duration of the time step. Thus, our model does not attempt to produce physically realistic solutions; instead we focus on qualitative accuracy from a simple model. In the following, we simplify the notation by dropping the subscript t.

From assumptions (2) and (5), the flow among the epidermal water compartment in location i and its neighbours is equal to the sum of the gradients (the differences in water potential between two compartments) multiplied by the hydraulic conductance (L):

$$F_e^i = \sum_{j=1}^{n} L(\Psi_e^j - \Psi_e^i) = Ln(\Psi_e^n - \Psi_e^i), \tag{3}$$

where the superscript j refers to one of n neighbouring epidermal compartments, where n is determined by the position of i in the lattice (not the areole; Fig. 1). Interior SUs have eight neighbours; SUs on boundaries have fewer neighbours. Finally, since the units of time are arbitrary in a finite difference model, we convert and scale water flow units (Eqn 3) to water potential units by multiplying by a (Eqn 1) and setting $c = La$.

Assuming boundary layer resistance to be negligible, the transpiration rate E (Eqn 1) is the product of stomatal conductance (g) and the water mole fraction difference between the leaf and air (Δw):

$$E^i = g^i \Delta w. \tag{4}$$

Stomatal conductance (g) is proportional to the stomatal aperture (A):

$$g^i = qA^i, \tag{5}$$

where q is an empirical scaling factor.

By assumption (1), stomatal aperture is proportional to the turgor pressures of the guard and epidermal cells:

$$A^i = \begin{cases} C_g^i P_g^i - C_e^i P_e^i & \text{if } C_g^i P_g^i > C_e^i P_e^i \\ 0 & \text{otherwise} \end{cases} \quad (6)$$

where C_g^i and C_e^i are the mechanical influence coefficients (Sharpe *et al.* 1987) of the guard and epidermal cells, respectively, in the ith SU, and P_g^i and P_e^i are the turgor pressures of the guard and epidermal cells, respectively, in the ith SU. This equation has been used in previous models of stomatal functioning (Cowan 1972; Delwiche & Cooke 1977), and it was formally derived by Cooke *et al.* (1976).

Turgor pressures for the guard and epidermal cells were calculated from their water potentials and osmotic pressures:

$$P_g^i = \begin{cases} \Psi_g^i - \pi_g^i & \text{if } \pi_g^i < \Psi_g^i \\ 0 & \text{otherwise} \end{cases} \quad (7)$$

where π_g^i is guard cell osmotic pressure. P_e^i was calculated using a similar equation. The osmotic pressure (π_e^i) of the epidermis was assumed to be constant. As stated in assumption (4), epidermal turgor metabolically controlled π_g^i. Increased epidermal turgor causes solutes to be pumped into the guard cell and vice versa. To implement this concept, we assumed that P_e^i determined the steady-state value of π_g^i (denoted $\pi_g^{i,ss}$). We assumed that epidermal turgor could vary between zero and a maximum value equal to $-\pi_e^i$ and that π_g^i could vary between minimum and maximum values defined by input parameters (Table 1). The dependence of the steady-state value of π_g^i on P_e^i was:

$$\pi_g^{i,ss} = \pi_g^{min} + \left(\frac{P_e^i}{P_e^{max}} \right) \left(\pi_g^{max} - \pi_g^{min} \right), \quad (8)$$

where π_g^{max} and π_g^{min} are the maximum and minimum guard cell osmotic pressures, respectively, and P_e^{max} is maximum P_e ($= -\pi_e$).

Guard cell osmotic pressure was modelled to approach its steady-state value at a rate proportional to the difference between the current π_g^i and its steady-state value as follows:

$$\frac{d\pi_g^i}{dt} = \alpha \left(\pi_g^{i,ss} - \pi_g^i \right). \quad (9)$$

Lastly, we assumed that guard cell water potential was in equilibrium with epidermis water potential ($\Psi_g^i = \Psi_e^i$). After Eqn 9 is converted to finite difference form, it and Eqn 2 are iterated in parallel to solve the model.

Parameters and model experiments

Table 1 lists the definitions and nominal values of the model parameters. In addition to these parameters, the model also permits different numbers of stomatal units per areole, and different total numbers of veins per leaf. Initial values for P and π of the guard and epidermal cells were chosen from literature data (Meidner & Edwards 1975; Nonami & Schulze 1989), or, in some model runs, at random from within the ranges delimited by their user-defined extrema (see below). For the runs reported here, at $t = 0$, $\Psi_e = \Psi_g = -0.75$ MPa, $\pi_g = -2.25$ MPa, and $\pi_e = -1.5$ MPa (a constant). The water potential of the veins was maintained at zero, and π_g ranged from -1.5 to -3.0 MPa (π_g^{max} to π_g^{min}, Eqn 8). Initial testing of the model showed that these values affected the quantitative output of the model, but had very little or no effect on the qualitative nature of the output.

Values for α and c were more difficult to obtain from literature data because they represent complex combinations of kinetic parameters. The value of α reflects the rate of ion pumping into and out of the guard cell (Eqn 9), and the value of c represents the average hydraulic conductivity between adjacent epidermal compartments. Both of these parameters are relative to the time step of the model, and since time was not explicitly represented in the finite dif-

Table 1. Model parameters and nominal values used in simulations

Variable	Definition	Nominal
c	hydraulic conductivity time consultant	0.8
C_g	guard cell mechanical advantage	1.0
C_e^{min}	minimum epidermis mechanical advantage	1.35
C_e	modal epidermis mechanical advantage	1.56
C_e^{max}	maximum epidermis mechanical advantage	2.0
θ	C_e/C_g	variable
q	scaling factor between stomatal aperture and stomatal conductance	1.0
Δw	mole fraction difference ($\times 10^{-3}$) between the leaf interior and the ambient air	variable
π_e	epidermis osmotic pressure (MPa)	-1.5
π_g^{min}	minimum guard cell osmotic pressure (MPa)	-3.0
π_g^{max}	maximum guard cell osmotic pressure (MPa)	-1.5
P_c^{max}	maximum epidermis turgor pressure (MPa)	1.5
α	ion pumping time constant	0.1

ference equations, the absolute values of α and c affected only the time resolution of the model. The ratio of these two parameters was found to have a large effect on the behaviour of the model. In the absence of experimental data for these parameters, their values were chosen such that model output resembled data from leaves.

The most interesting and important parameter for the functioning of the model was the ratio of the influence coefficients (C_g and C_e, Eqn 6) for guard and epidermal turgor pressures on stomatal aperture. The absolute values of these coefficients were important only in relation to other values in the model. However, the ratio C_e/C_g was found to be important for the qualitative behaviour of the model; it was termed the 'mechanical advantage of the epidermis' (DeMichele & Sharpe 1973) and is here denoted by the symbol θ. In general, we found that high values of θ (> 1.6) caused stomata to oscillate in our model. Although this parameter has been set to 1.0 in some models (Dewar 1995), experimental data (Meidner & Edwards 1975) and theoretical results (Cooke *et al.* 1976) suggest that the average value of θ is ≈ 1.5. Furthermore, the analysis of Sharpe *et al.* (1987) suggests that it can vary among plants and even among stomata on a given leaf. To simulate this latter phenomenon, we assigned values of θ to individual stomatal units by randomly drawing values from a triangular probability density function. The locations of the peak and end points of this distribution were variable parameters; unless otherwise specified, we used end points of 1.35 and 2.0 and a peak of 1.6. Other randomizations (e.g. of the guard cell biochemical parameters) can and should be done in the future, but our preliminary model runs informed us that θ was a particularly sensitive parameter.

RESULTS

Simulations with spatially uniform parameters

When all stomatal units were assigned identical parameters and initial conditions, all areoles behaved identically. Depending on parameter values, the conductance of each individual stoma either reached a steady-state value or exhibited damped or sustained oscillations. In general, oscillations were produced by high values of Δw and/or θ. Although all stomata in an areole oscillated, they oscillated slightly out of phase, and at the level of the areole, oscillations were manifested as symmetric waves of high conductance emanating from the veins to the centre of each areole. With parameters that produced stable values of conductance, the conductance of any given stomatal unit was constant over time, but stomata near veins had higher steady-state conductance than those near the centre of an areole.

To determine the effect of θ and α on conductance oscillations, we varied θ at different values of α and measured the number of iterations required to reduce the oscillations to one-half of their original amplitude (Fig. 2). These data show the strong sensitivity of oscillatory behaviour on θ and α. When the rate of ion pumping is low (($= 0.1$), there
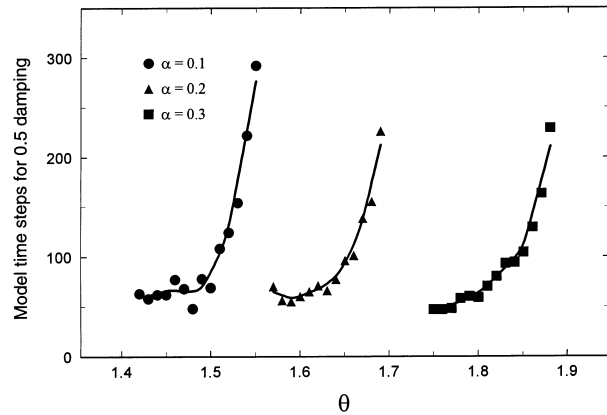
Figure 2. The effect of θ (epidermis mechanical advantage) on damping of stomatal oscillations. The uniform-θ model was run for a single areole with random starting values for the epidermal Ψ of each stomatal unit. The ordinate axis shows the number of model time steps required for stomatal conductance oscillations to damp to one-half of the original amplitude. Model responses for three levels of biochemical pumping rates (α) are shown.

is a long time lag for π_g to equilibrate to π_g^{ss}, the level set by P_e. This results in a transition from rapidly damped oscillations to sustained oscillations at relatively low values of θ. When α is large, the time lag is short, π_g equilibrates quickly, and a greater mechanical advantage (θ) is required to induce oscillations.

Simulations with spatially randomized parameters

To produce spatial heterogeneity in the model, we assigned random values of C_e to individual stomata based on a triangular distribution, as described in the 'Materials and methods' section. At low and moderate values of Δw for which conductance reached a steady state, this produced random heterogeneity in conductance among stomata. However, the variation in conductance was not large, either among stomatal units or among areoles (Fig. 3, inset). At these values of Δw, the average steady-state modelled leaf conductance declined hyperbolically with increasing Δw (Fig. 3) and declined with increasing transpiration rate in a linear fashion (Fig. 4). This general response is similar to data reported for leaves (reviewed in Monteith 1995), and is illustrated for a *Xanthium strumarium* leaf in Fig. 3.

The kinetics predicted by the model for humidity responses were also similar to data from real leaves. This is illustrated in Fig. 5, which shows modelled leaf average conductance for a step increase in Δw from 5 to 15 as well as data for a leaf of *Triticum aestivum* L. subjected to a step increase in Δw from 9 to 18 Pa Pa^{-1}. In both cases, stomatal conductance increased transiently before decreasing to a lower steady-state conductance. For a step decrease in Δw, the model predicted a transient decrease in stomatal conductance, followed by a gradual increase to a higher steady-state value (not shown). Data from leaves show a similar response (not shown).
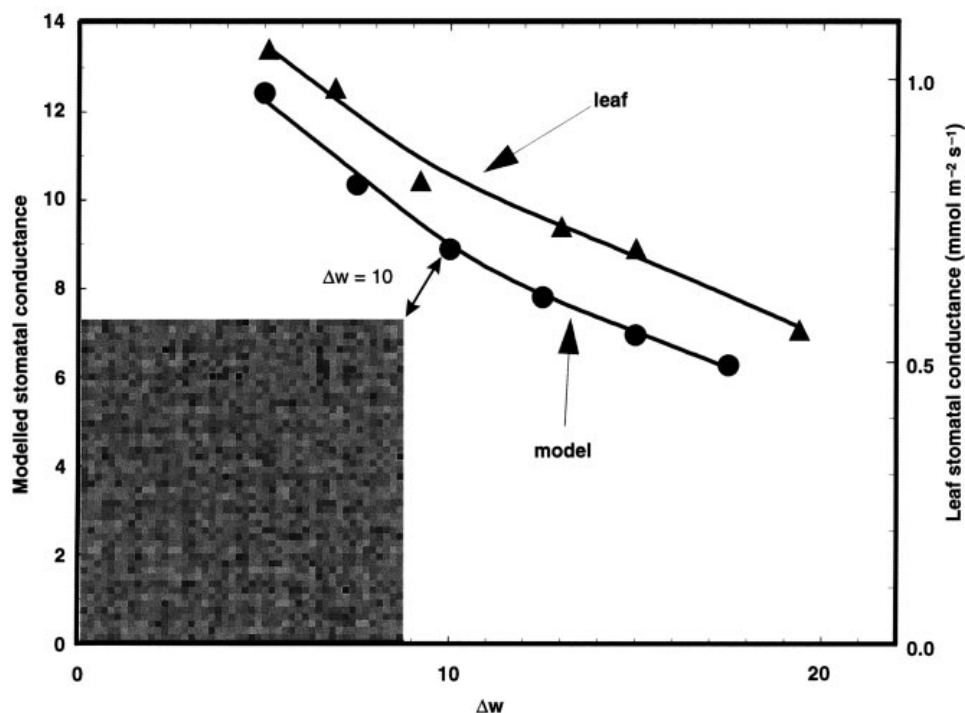
Figure 3. Response of steady-state stomatal conductance to Δw for the model and a leaf of *Xanthium strumarium*. The inset shows the spatial distribution of stomatal conductance for the model at a Δw value of 10; spatial distributions at other values of Δw were similar. Each square represents a stomatal unit, and each areole is 4×4 stomatal units; lighter greyscales correspond to lower conductance values. The data for *Xanthium* were obtained at a leaf temperature of 25 °C, a CO_2 concentration of 350 μmol mol^{-1}, an O_2 concentration of 0·21 mol mol^{-1}, and a PFD of 1000 μmol m^{-2} s^{-1}. The lines are non-linear regressions.

At higher Δw values (for which stomatal conductance oscillated in simulations with uniform parameters), the effects of spatial variation in θ were much more pronounced. The critical Δw value inducing oscillations differed among areoles, but all of the stomata in a given areole either oscillated in phase or were stable. Each oscillating areole had its own characteristic amplitude and period of oscillation, and after sufficient time had elapsed for these oscillations to become out of phase, a 'patchy' distribution of conductance emerged in which, for any given time step, some areoles had mostly closed stomata while others had mostly open stomata. These complex temporal and spatial patterns of conductance qualitatively resembled those observed in leaves at high values of Δw (Cardon *et al.* 1994; Siebke & Weis 1995). This result is illustrated in Fig. 6, which shows model output and data from a *Xanthium* leaf at high Δw. In both cases, individual areoles show oscillatory behaviour with varied periods and amplitudes, but the average stomatal conductance of the leaf is relatively stable. To investigate the tendency of stomata within an areole to self-organize, we ran the model at high Δw with random initial values for Ψ_g and π_g and plotted the dynamics of conductance for each stomatal unit in a single areole (Fig. 7a). Despite widely differing values of conductance at time zero (because of the random initial conditions), all the stomata in the areole eventually converged to one of three modes. These three modes existed because stomatal units in a four-by-four rectangular areole can be in three positions relative to veins: in a corner of the areole,

on a side, or in the middle as illustrated in the inset diagram. All three positions have the same number of neighbours (eight), but these neighbours have different dynamics. For example, a corner SU has five neighbours that are veins, whose water potential is by assumption constant. Similarly, SUs on the side of the areole have three vein neighbours and the interior SUs have no vein neighbours.
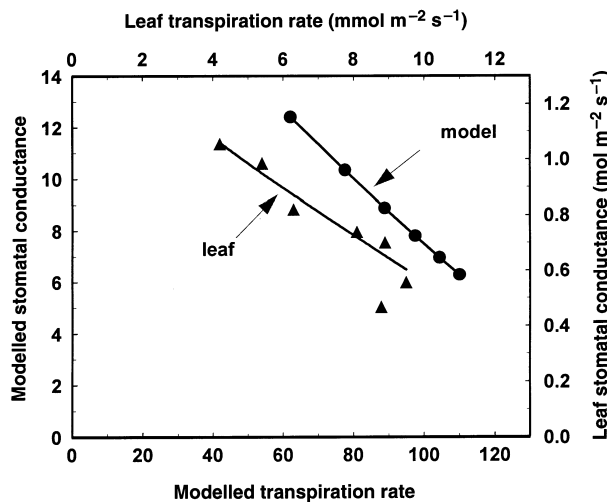
Figure 4. Data from Fig. 3 replotted as the response of steady-state stomatal conductance to transpiration rate. The lines are linear regressions; the lowest conductance point for the leaf was not included in its regression.
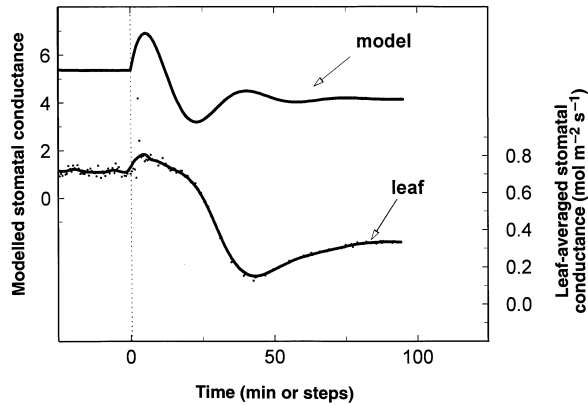
Figure 5. Responses of stomatal conductance to increase in Δw for the model and for a leaf of *Triticum aestivum* L. In the model, the parameter Δw was increased from 5 to 15 units at $t = 0$; in the leaf Δw was increased from 9 to 18 Pa Pa^{-a} at $t = 0$. Data for the leaf were obtained at a CO_2 concentration of 350 μmol mol^{-1}, a leaf temperature of 25 °C, an O_2 concentration of 0·21 mol mol^{-1}, and a PFD of 900 μmol m^{-2} s^{-1}.

This convergence of stomatal dynamics is remarkable not only because of the random starting values, but also because several stomata in the areole had values of θ which, in the homogeneous model, *would have induced stomatal oscillations*. The behaviour of one such stoma, having a θ value of 1·867, is identified by a dotted line in Fig. 7a. Figure 7b shows the behaviour of the model when this value for θ is assigned to all SU in the areole, with random starting values for Ψ_g and π_g. Again the stomata converged on three values corresponding to the three positions in the areole, but in this case all stomata showed undamped, synchronous oscillations. Thus, the stoma with $\theta = 1·867$, indicated by the dotted line in Fig. 7a, was 'coerced' into non-oscillatory behaviour by other stomata in the same areole, despite its oscillatory value of θ.

The tendency for stomatal behaviour to become coordinated within an areole was further investigated by altering the model to maintain Δw constant for the central stoma in a single areole while causing the surrounding units to experience an increase in Δw. To approximate more closely the experimental test (see Mott *et al.* 1997, accompanying paper), Δw values for the surrounding stomatal units were made to increase in an exponential fashion with distance from the central stomatal unit. Figure 8 shows that, despite experiencing no change in Δw, the central stoma responded to the perturbation experienced by its neighbours. This response was almost indistinguishable from that of its neighbours, which experienced the Δw perturbation directly.

DISCUSSION

The portions of our model describing the operation of individual stomata were similar to previous models of stomatal functioning (Cowan 1972; Delwiche & Cooke 1977; Dewar 1995), and produced qualitatively similar results for a single

stoma (data not shown). We have gone beyond these models by incorporating an effect of epidermal turgor on guard cell osmotic pressure. Moreover, by modelling stomata as coupled hydraulic units in a two-dimensional lattice, our study provides insights into stomatal responses to humidity in intact leaves that are not evident from models of individual stomata. A similar approach was taken by Rand *et al.* (1982) and Rand & Ellenson (1986), who linearized the single stoma model of Delwiche & Cooke (1977) to facilitate mathematical analysis. Their model, which did not incorporate veins or guard cell osmotic pressure dynamics, showed that stomata could open in waves across the leaf, and they presented evidence that such waves of stomatal opening did occur in leaves under some circumstances. By including veins in our model, we effectively divided the leaf into independently functioning hydraulic units corresponding to the areoles of a leaf. These modelled areoles behaved identically when parameters were identical for all stomata, and under oscillatory conditions (high Δw) they showed waves of stomatal opening similar to those of Rand & Ellenson (1986). However, when the mechanical advantage of the epidermal cells (θ) was varied randomly among individual stomatal units, the model showed complex spatial and temporal patterns similar to those observed in leaves at high values of Δw (Cardon *et al.* 1994; Siebke & Weis 1995).

Our model, like all others, makes a number of assumptions to which the results could be sensitive. For example, we hypothesized that the observed spatial patterns were caused by local, hydraulic interactions among SUs, rather than a large-scale signal propagating over the leaf surface. This latter suggestion is an interesting idea that is worth modelling. It is very possible that a combination of local and global mechanisms will be needed to portray the spatial patterns accurately. We also assumed that the boundary layer resistance was zero, which is false in some cases. This may be important since an additional resistance will tend to dampen stomatal oscillations, thereby requiring larger Δw to induce the dynamics we report. Our model also assumes linear relations in several cases (e.g. aperture as a function of guard cell and epidermis turgor, or epidermis water potential as a function of water flux from neighbours and transpiration losses). Relaxing these assumptions may alter our conclusions, but the linear model is an appropriate starting point.

Because it was difficult to obtain values for many of the model parameters, we have not interpreted the results of our model quantitatively. However, most parameters could be varied over a moderate range without affecting the qualitative behaviour of the model. It is these qualitative aspects of the model's output that are discussed below.

An important qualitative prediction of the model is that, for low and moderate values of Δw, stomatal conductance varied linearly with transpiration rate and therefore hyperbolically with Δw (Figs 3 & 4). Both versions (uniform θ and non-uniform θ) of the model showed this response. For uniform θ the conductance of a particular stomatal unit was uniquely related to its position in the areole, and all areoles behaved identically. With spatially randomized θ the distribution of stomatal conductances within each areole was

(a)

(b)
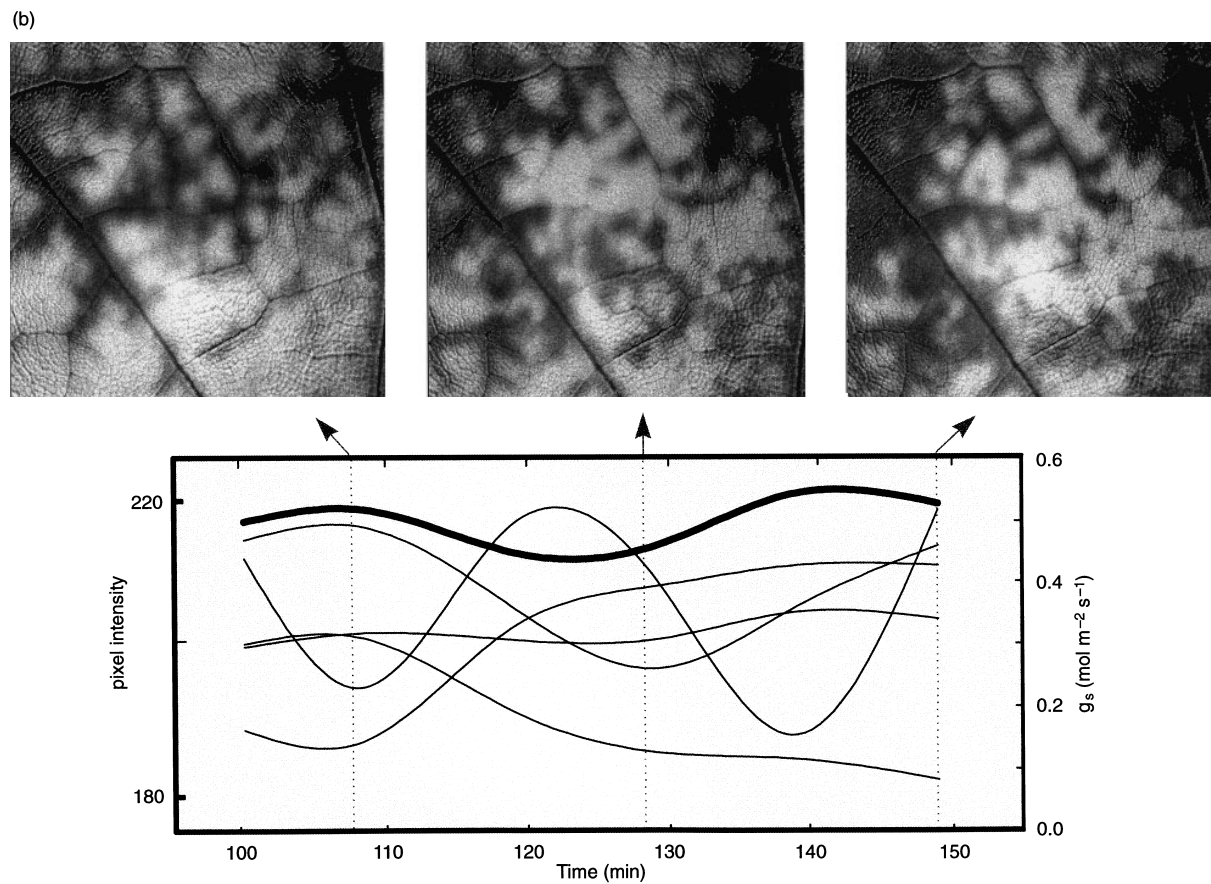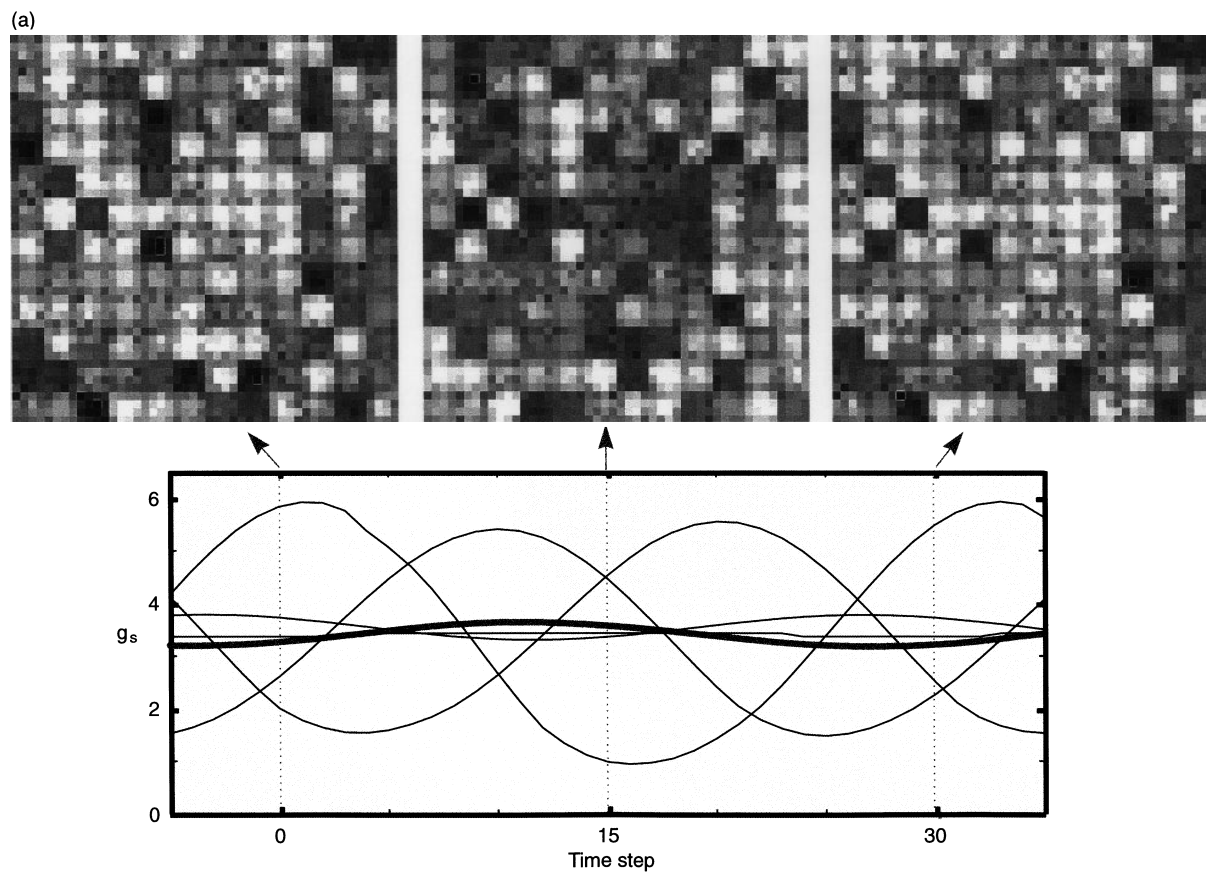
slightly different, but there was no substantial difference in the average conductance among areoles (Fig. 6a). Monteith (1995) showed that conductance responds linearly to transpiration rate in many species and that this response is a consequence of a feedback regulation of stomatal conductance to transpiration rate. In our model, the linear relationship between stomatal conductance and transpiration was caused by the linear dependence of $\pi_g^{i,ss}$ on epidermal turgor pressure (Eqn 8), but other mechanisms can produce similar responses (Dewar 1995).

The kinetics of stomatal responses to a change in Δw were also correctly predicted by the model with both uniform and random distributions of θ. These kinetics were characterized by an initial transient response in the direction opposite to the steady-state response, followed by a slower approach to the new steady-state value. This general response has been discussed in the literature (e.g. Cowan 1972; Cowan 1977; Schulze 1994), and has been shown to represent a true change in stomatal aperture (Kappen & Haeger 1991).

At high values of Δw, modelled stomatal conductance oscillated. In our model, oscillations were caused by a time lag between the response of epidermal turgor to changes in stomatal conductance and the response of guard cell osmotic pressure to changes in epidermal turgor. At high Δw, the effect of stomatal aperture on transpiration rate is large, and at high values of θ the effect of epidermal turgor on stomatal conductance is large. Therefore, both of these conditions (high Δw and high θ) favoured oscillatory behaviour. In earlier models, oscillations resulted from a lag in the hydraulic equilibrium between guard and epidermal cells (Cowan 1972). However, the available evidence supports an active change in the osmotic concentration of guard cells during humidity responses (Losch & Schenk 1978), and there is little evidence for a very low hydraulic conductivity between epidermal and guard cells (Cowan 1977).

The sensitivity of stomatal dynamics to the mechanical advantage of the epidermis (θ) has been noted in previous models of a stoma (Delwiche & Cooke 1977), and our study reinforces the importance of this parameter for stomatal functioning in leaves. The theoretical analysis of Sharpe *et al.* (1987) shows that θ is a function of guard and epidermal cell dimensions, and it therefore seems possible that the value of θ could vary substantially among species and among individual stomata on a single leaf. Our model shows that random variation in θ among the stomata of a single leaf can have large effects on the functioning of stomata at high values of Δw.

Although θ is technically difficult to measure, it has been estimated for *Tradescantia virginiana* to be between 1·6 and 2·0 (Meidner & Edwards 1975; Meidner & Bannister 1979). These data are consistent with a theoretical analysis (Cooke *et al.* 1976) that suggested a value of about 1·5. Other models (Dewar 1995) and data (Stalfelt 1966) have suggested a value closer to 1·0, and Dewar (1995) postulates that this inconsistency may be because the mechanical advantage of the epidermis falls off with distance from the guard cells. This is undoubtedly true, but in the absence of large gradients in π, Ψ or wall elasticity within the epidermis, changes in turgor caused by changes in transpiration rate should be similar throughout the epidermis. Since the relevant mechanical interactions will be those between the guard cells and the immediately adjacent epidermal cells, the relevant mechanical advantage will be that which applies to these cells. We therefore used values of θ between 1·3 and 2·0 as suggested by the literature data. Given the importance of this parameter to stomatal functioning, more detailed measurements from a wider variety of species are clearly needed.

One of the most important results of this study is the effect of random spatial heterogeneity in the mechanical advantage of the epidermal cells (θ) on spatial patterns of stomatal conductance at high values of Δw. At low values of Δw, a spatially random distribution of θ produced only small, random differences in conductance among stomata. At high values of Δw, however, random variation in θ among stomata caused the critical value of Δw inducing oscillations to differ among areoles. Stomatal behaviour thus became coordinated at the scale of the areole, but uncoordinated at the scale of the leaf. As a result, the spatial and temporal patterns of stomatal conductance produced by the model at high values of Δw were similar to the 'patchy' patterns observed in leaves under similar conditions (e.g. Figs 5 & 6). Future models that incorporate localized drawdown of Ψ in veins, thus allowing for interaction among areoles, might show the large-scale structures (e.g. many patches oscillating together) that have been demonstrated in leaves (Cardon *et al.* 1994; Weis & Siebke 1995).

Because of the hydraulic coupling of the stomatal units in our model, stomata within a single areole tended to behave synchronously, and stomata could be 'coerced' into responses that they would not display in the absence of the effects of neighbouring stomata. This coercion effect could be either stabilizing or destabilizing. For example, an individual stoma with a supercritical value for θ (i.e. one which caused oscillations if shared by all stomata in an areole) did not oscillate when surrounded by stomata with lower values for θ (Fig. 7a). Conversely, if Δw was held constant for one stoma but varied for the surrounding stomata, hydraulic coupling produced a large effect on the stoma for which Δw was constant (Fig. 8).

Figure 6. Spatial and temporal dynamics of stomatal conductance associated with patchy stomatal movements induced by high Δw in (a) the model (areole size = 4×4 SUs), and (b) a leaf of *Xanthium strumarium* at $\Delta w = 20\cdot8$ and O_2 concentration of $0\cdot02$ mol mol^{-1}. Conductance time courses are accompanied in (a) by graphical images of the spatial variation in conductance from the model, and in (b) by fluorescence images of the leaf for which gas-exchange measurements were being taken. In both cases, brighter areas correspond to areas of higher stomatal conductance. The thin lines for both (a) and (b) represent average conductance for several selected areoles over time (determined explicitly for the model and inferred from pixel intensity for the leaf). The single thick line in each graph shows the average leaf conductance (determined explicitly for the model, and by gas-exchange measurements for the leaf).
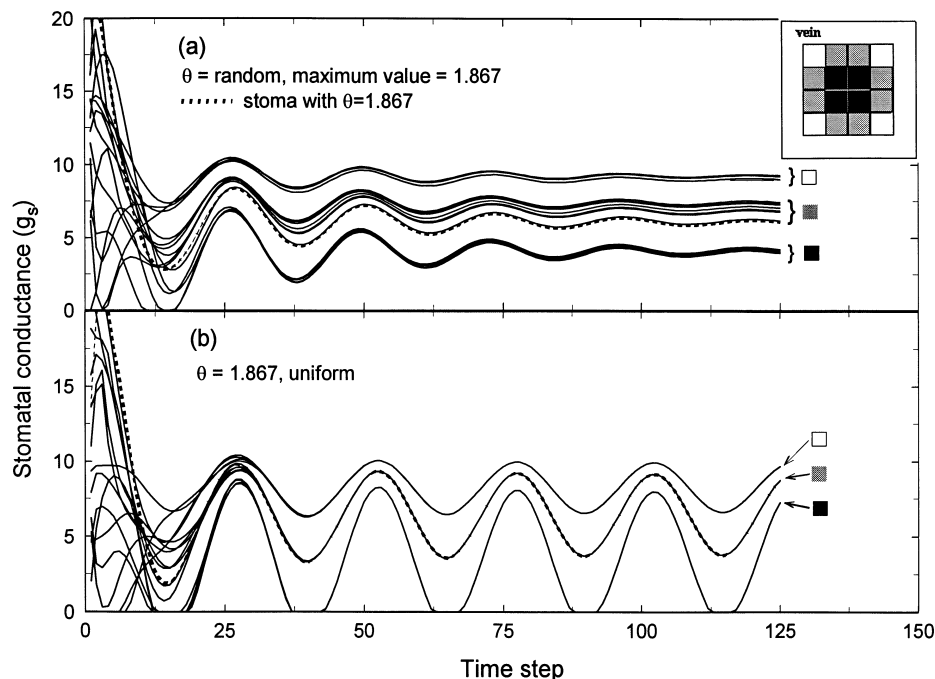
Figure 7. Stomatal conductance (g_s) versus time step for each of 16 stomata within an areole when the Ψ and π values for each stoma were assigned random initial values. In (a), random values for the mechanical advantage (θ) were assigned based on a triangular relative frequency distribution function with range [1·35, 2·0] and mode 1·6. The maximum value of θ for this areole was 1·867, and the stoma with $\theta = 1·867$ is plotted with a dashed line. In (b), an otherwise identical areole with θ uniformly equal to 1·867 is plotted, showing that this value for θ should lead to sustained oscillations. However, the presence of neighbouring stomata with lower values for θ in (a) exerted a controlling influence, overriding the oscillatory tendencies of the stoma with $\theta = 1·867$. Stomatal behaviour is seen to converge to three basic modes, corresponding to the three possible topologically distinct positions (in terms of proximity to a vein) for stomata within a 4 × 4 areole. These positions are indicated by differently coloured boxes in the inset diagram of an areole (a), and placed next to the end of the time courses in both (a) and (b). (Empty boxes correspond to stomata in the corners of the areole, bordered on two sides by veins; grey boxes indicate stomata bordered by a single vein, and solid boxes indicate stomata in the centre of the areole.) The variability in steady-state conductance for stomata at similar positions in (a) is due to their different, randomly assigned values for θ.
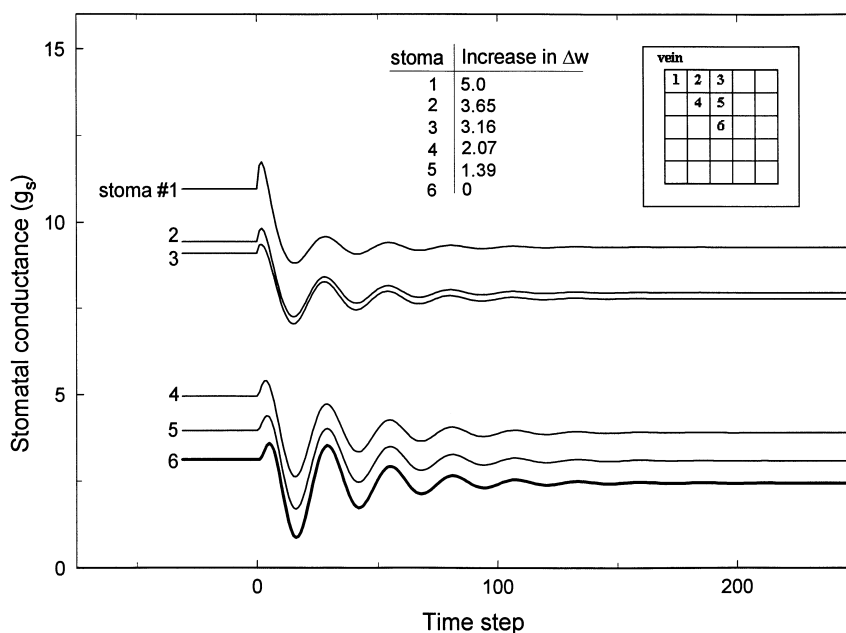
Figure 8. Stomatal conductance (g_s) plotted for six stomata following an increase in Δw from an initial value of 10. The amount by which Δw changed increased exponentially from 0 to 5 with increasing distance from the centre of the areole. Changes in Δw experienced by each stoma are described in the inset areole diagram and table. Although the stoma marked as '6' in the inset areole diagram experienced no change in Δw, it showed a large response to the perturbation of Δw in the surrounding stomatal units.

These results suggest that the same mechanism responsible for coordinating stomatal behaviour within each areole may also have been responsible for causing stomatal behaviour to become uncoordinated among areoles. Given the broad range of behavioural modes exhibited by different areoles when θ was spatially randomized, it seems likely that in many areoles a number of stomata with relatively extreme values for θ may have 'coerced' their neighbours into a particular mode of behaviour. The extreme values of θ that may determine each areole's behaviour in this way (by coercion) would differ among areoles, and the resulting diversity of amplitudes and periods of oscillation would lead to the observed uncoordination of stomatal behaviour among areoles. This coercion (exemplified in Figs 7 & 8) acts by the same mechanism of hydraulic coupling that serves to coordinate stomatal behaviour within each areole.

The prediction that one stoma can be coerced to respond to humidity perturbations experienced only by its neighbours (Fig. 8) suggested a testable hypothesis concerning the hydraulic interactions incorporated in our model. This led to a series of experiments analogous to the simulation represented in Fig. 8. The data from these experiments are described in the study following this one.

ACKNOWLEDGMENTS

REFERENCES

Ball J.T., Woodrow I.E. & Berry J.A. (1987) A model predicting stomatal conductance and its contribution to the control of photosynthesis under different environemtnal conditions. In *Progress in Photosynthesis Research* (ed. I. Biggins), pp. 221–224. Marinus Nijhoff Publishers, Netherlands.

Bro E., Meyer S. & Genty B. (1996) Herogeneity of leaf CO_2 assimilation during photosynthetic induction. *Plant, Cell and Environment* **19**, 1349–1358.

Cardon Z.G, Mott K.A. & Berry J.A. (1994) Dynamics of patchy stomatal movements, and their contribution to steady-state and oscillating stomatal conductance calculated with gas-exchange techniques. *Plant, Cell and Environment* **17**, 995–1008.

Cooke J.R., De Baerdemaeker J.G., Rand R.H. & Mang H.A. (1976) A finite element shell analysis of guard cell deformations. *Transactions of the ASAE* **19**, 1107–1121.

Cowan I.R. (1972) Oscillations in stomatal conductance and plant functioning associated with stomatal conductance: Observations and a model. *Planta* **106**, 185–219.

Cowan I.R. (1977) Stomatal behaviour and environment. *Advances in Botanical Research* **4**, 117–228.

Daley P.F., Raschke K., Ball J.T. & Berry J.A. (1989) Topography of photosynthetic activity o fleaves obtained from video images of chlorophyll fluorescence. *Plant Physiology* **90**, 1233–1238.

Delwiche M.J. & Cooke J.R (1977) An analytic model of the hydraulic aspects of stomatal dynamics. *Journal of Theoretical Biology* **69**, 113–141.

DeMichele D.W. & Sharpe P.J.H. (1973) An analysis of the mechanics of guard cell motion. *Journal of Theoretical Biology* **41**, 77–96.

Dewar D.C. (1995) Interpretation of an empirical model for stomatal conductance in terms of guard cell function. *Plant, Cell and Environment* **18**, 365–372.

Kappen L. & Haeger S. (1991) Stomatal responses of *Tradescantia albiflora* to changing air humidity in light and in darkness. *Journal of Experimental Botany* **42**, 979–986.

Laisk A. (1980) Statistical distribution of stomatal apertures of *Vicia faba* and *Hordeum vulgare* and the *Spannumgsphase* of stomatal opening. *Journal of Experimental Botany* **31**, 49–58.

Leuning R. (1995) A critical appraisal of a combined stomatal-photosynthesis model for C_3 plants. *Plant, Cell and Environment* **18**, 339–355.

Losch R. & Schenk B. (1978) Humidity response of stomata and the potassium content of guard cells. *Journal of Experimental Botany* **29**, 781–787.

Meidner H. & Edwards M. (1975) Direct measurements of turgor potentials of guard cells, I. *Journal of Experimental Botany* **26**, 319–330.

Meidner H. & Bannister J. (1979) Pressure and solute potential in stomatal cells of *Tradescantia virginiana*. *Journal of Experimental Botany* **30**, 255–265.

Monteith J.L. (1995) A reinterpretation of stomatal responses to humidity. *Plant, Cell and Environment* **18**, 357–364.

Mott K.A. (1995) Effects of patchy stomatal closure on gas-exchange measurements following abscisic acid treatment. *Plant, Cell and Envionment* **18**, 1291–1300.

Mott K.A. & Parkhurst D.F. (1991) Stomatal responses to humidity in air and helox. *Plant, Cell and Environment* **14**, 509–515.

Mott K.A., Cardon Z.G. & Berry J.A. (1993) Asymmetric patchy stomatal closure for the two surfaces of *Xanthium strumarium* L. leaves at low humidity. *Plant, Cell and Environment* **16**, 25–34.

Mott K.A., Denne F. & Powell J. (1997) Interactions among stomata in response to perturbations in humidity. *Plant, Cell and Environment* **20**, 1098–1107.

Nonami H. & Schulze E.-D (1989) Cell water potential, osmotic potential, and turgor in the epidermis and mesophyll of transpiring leaves. *Planta* **177**, 35–46.

Pospisilova J. & Santrucek J. (1994) Stomatal patchiness. *Biologia Plantarum* **36**, 481–510.

Rand R.H. & Ellenson J.L. (1986) Dynamics of stomate fields in leaves. *Lectures on Mathematics in the Life Sciences* **18**, 51–86.

Rand R.H., Storti D.W., Upadhyaya S.K. & Cooke J.R. (1982) Dynamics of coupled stomatal oscillators. *Journal of Mathematical Biology* **15**, 131–149.

Schulze E.-D. (1994) The regulation of plant transpiration: Interactions of feedforward, feedback, and futile cycles In *Flux Control in Biological Systems* (ed. E. -D. Schulze), pp. 203–235. Academic Press, Inc., San Diego.

Shackel K.A. & Brinckmann E. (1985) In situ measurement of epidermal cell turgor, leaf water potential, and gas exchange in *Tradescantia virginiana* L. *Plant Physiology* **78**, 66–70.

Sharpe P.J, Wu H., Spence R.D. (1987) Stomatal Mechanics. In *Stomatal Mechanics* (ed. E. Zeiger, G. D. Farquhar & I. R. Cowan), pp. 91–114. Stanford University Press, Stanford.

Siebke K. & Weis E. (1995) 'Assimilation images' of leaves of *Glechoma hederacea*: Analysis of non-synchronous stomata related oscillations. *Planta* **196**, 155–165.

Stalfelt M.G. (1966) The role of the epidermal cells in the stomatal movements. *Physiologia Plantarum* **19**, 241–256.

Terashima I. (1992) Anatomy of non-uniform photosynthesis. *Photosynthesis Research* **31**, 195–212.

Weis E. & Siebke K. (1995) Imaging of chlorophyll fluorescence in leaves: Topography of photosynthesis oscillations in leaves of *Glechoma hederacea*. *Photosynthesis Research* **45**, 225–237.